Enhanced Optics for Time-Resolved Singlet Oxygen Luminescence Detection

Konstantinos Tsimvrakidis, Nathan R. Gemmell, Kleanthis Erotokritou, Shigehito Miki, Masahiro Yabuno, Taro Yamashita, Hirotaka Terai, and Robert H. Hadfield, *Senior Member, IEEE*

***Abstract*—Singlet oxygen luminescence dosimetry (SOLD) is a highly promising direct monitoring method for photodynamic therapy (PDT) in the treatment of cancer. Early SOLD systems have been hampered by inefficient excitation, poor optical collection and immature infrared single photon detection technology. We report carefully engineered improvements addressing all of these deficiencies. We use a supercontinuum source with a tunable filter to precisely target the peak absorption wavelength of the chosen photosensitizer; we have designed a compact and versatile optical package for precise alignment; we have successfully employed state-of-the-art superconducting photon counting technologies. Through these improvements, we can achieve histogram acquisition from a photosensitizer in solution test sample. This setup opens the pathway to physiological SOLD studies for PDT dosimetry.**

***Index Terms*—Photochemistry, solution test, superconducting photodetectors, fluorescence spectroscopy, laser biomedical applications.**

I. Introduction

SINGLET oxygen ($^1O_2$), is the electronic excited state ($^1O_2(a\ ^1\Delta_g)$) of molecular oxygen which has by default its electronic ground state in a spin triplet state ($^3O_2(X\ ^3\sum_g^-)$) [1]. Singlet oxygen is a main component in many biological processes, and in photodynamic therapy (PDT) cancer treatments, it acts as the cytotoxic agent [1], [2]. In PDT, singlet oxygen is generated via a photosensitized method, consisting of an illumination source of specific wavelength, a Type II photosensitizer (PS, a dye molecule) and molecular oxygen [3].

Manuscript received March 29, 2018; revised May 7, 2018; accepted May 8, 2018. Date of publication May 22, 2018; date of current version June 14, 2018. This work was supported by the UK Engineering and Physical Sciences Research Council via the QuantIC quantum technology hub in quantum enhanced imaging under Grant EP/M01326X/1. The work of R. H. Hadfield was supported by a European Research Council Consolidator under Grant IRIS 648604. *(Corresponding author: Konstantinos Tsimvrakidis.)*

K. Tsimvrakidis, K. Erotokritou and R. H. Hadfield are with the Department of Electronics and Nanoscale Engineering, University of Glasgow, Glasgow G12 8QQ, U.K. (e-mail: k.tsimvrakidis.1@research.gla.ac.uk; k.erotokritou.1@research.gla.ac.uk; Robert.Hadfield@glasgow.ac.uk).

N. R. Gemmell is with the University of Sussex, Brighton BN1 9RH, U.K. (e-mail: N.Gemmell@sussex.ac.uk).

S. Miki and H. Terai is with the Nano ICT group, National Institute of Information and Communications Technology, Kobe 651-2492, Japan (e-mail: s-miki@nict.go.jp; terai@nict.go.jp).

M. Yabuno is with the Joho Tsushin Kenkyu Kiko Mirai ICT Kenkyu Center, Kobe 651-2492, Japan (e-mail: masahiro.yabuno@nict.go.jp).

T. Yamashita is with Nagoya University, Nagoya 464-8601, Japan (e-mail: yamashita@nuee.nagoya-u.ac.jp).

Color versions of one or more of the figures in this paper are available online at http://ieeexplore.ieee.org.

Digital Object Identifier 10.1109/JSTQE.2018.2836962

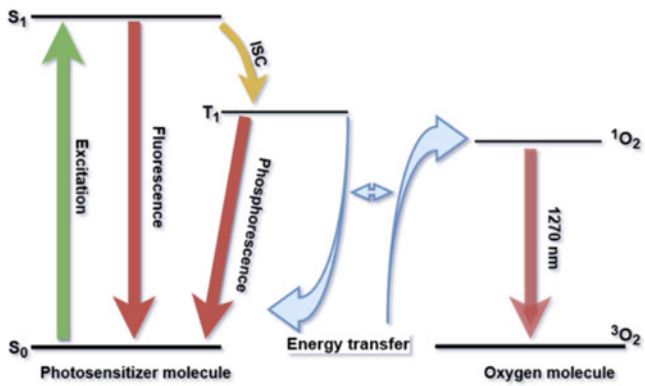

Fig. 1. Jablonski diagram illustrating the photosensitized generation and near-infrared 1270 nm emission of singlet oxygen ($^1O_2$). An illumination source of specific wavelength excites the Type II photosensitizer to an excited singlet state S_1. From this electronic energy level, the photosensitizer molecule can return to its ground state and undergo intersystem crossing, transferring energy to its triplet state T_1. From T_1 it can decay back to ground state by a long-lived phosphorescence and can transfer energy to oxygen molecules exciting each into a singlet state $^1O_2$. The decay from the singlet state to the ground state $^3O_2$, triggers the emission of a 1270 nm wavelength photon.

These three components, being individually harmless for living tissue, have a powerful effect when combined; light activates the photosensitizer compounds which undergo a photochemical process to produce singlet oxygen, causing local cell necrosis [4]. However, these components are interdependent in this process while also dependent on the physiological microenvironment in which treatment takes place. Factors such as blood flow, local tissue oxygenation and photobleaching, as well as local concentration or distribution of the photosensitizer all play a role, making efficient PDT dosimetry a very challenging task [5], [6]. In the pursuit of an efficient PDT dosimetry technique, a range of methodologies have been put forward, such as implicit dosimetry, explicit dosimetry and biophysical/biological tissue response monitoring [7]–[16]. Singlet Oxygen Luminescence Dosimetry (SOLD), which is a highly promising direct dosimetry method [7], [17], [18], [19], exploits the detection of the luminescent decay from singlet oxygen to the ground triplet state [7], [18], [20], as shown in Fig. 1. Such a direct dosimetry technique offers the key advantage that it requires only one parameter; the measurement of singlet oxygen luminescence in the near infrared at 1270 nm wavelength. While this is an ideal dosimetry technique, development of SOLD has proven quite challenging as the majority of the off-the-self single-photon

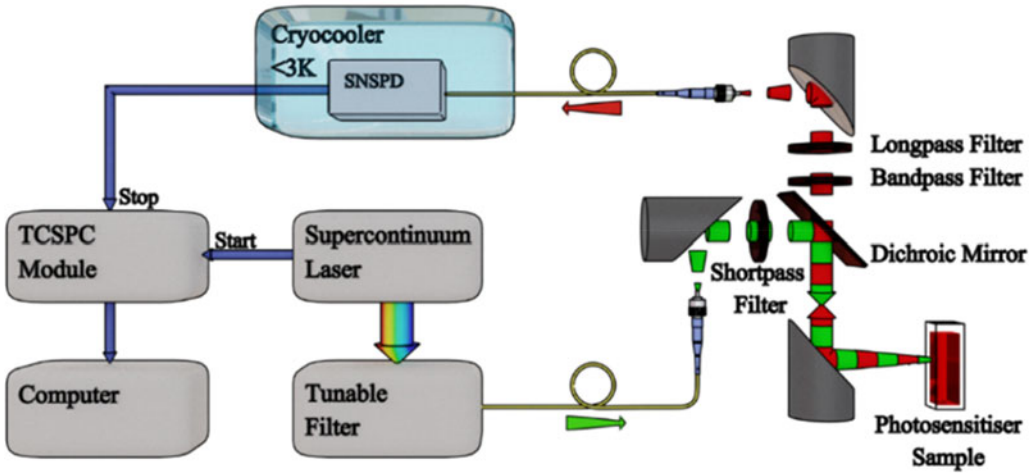

Fig. 2. Block diagram illustrating the Singlet oxygen luminescence detection experimental setup. The supercontinuum laser is coupled via a collimation package to the optical part of setup where the singlet oxygen generation process takes place and the 1270 nm photons emitted and collected in the collection collimation package which is coupled to the superconducting nanowire single-photon detector (SNSPD). With the supercontinuum laser giving a start signal and similarly the detector output a stop signal, time-correlated single-photon counting (TCSPC) is achieved.

detectors are not efficient enough in this spectral region and suffer from high dark counts [21]. Moreover, this specific decay has a very short lifetime (usually in nanoseconds *in vivo*) and low probability ($\sim 10^{-7}$) when interacting with biological media during the actual treatment [18], [19].

Nowadays, commercial singlet oxygen detection systems are available. These are large monochromator-based instruments incorporating IR PMTs and InGaAs SPADs, and due to not being fiber coupled, they cannot be easily implemented into a clinical PDT dosimetry system. Recently, we presented $^1O_2$ luminescence detection using a fixed wavelength laser (523 nm wavelength), an improvised collection optical setup and an early generation superconducting nanowire single-photon detector (SNSPD), followed by a gated InGaAs/InP single-photon avalanche diode (SPAD) detector [18], [19]. Here, we report a complete, advanced $^1O_2$ luminescence detection system using a supercontinuum laser coupled to a tunable filter making it ideal for exciting most of the photosensitizers available to date, an improved compact optical setup for the efficient delivery of the excitation light and the collection of the 1270 nm photons, and a SNSPD with high efficiency and tunable to sub-Hz dark count rate. With the SOLD system presented here, we have achieved efficient detection of $^1O_2$ signal on histograms with higher resolution (about 65 ns bin size over the old 1024 ns bin size histograms) using multiple photosensitizers in solution test samples, bringing SOLD a step closer to being incorporated as a valid dosimetry technique into PDT therapies.

II. Experimental Setup

The experimental setup for the singlet oxygen detection measurement is illustrated by a block diagram in Fig. 2. The illumination source for the excitation of the photosensitizer is a SuperK compact supercontinuum laser by NKT Photonics with wide spectral range from 450 nm to 2400 nm, $<$2 ns wide optical output pulses and a variable repetition rate up to 24 kHz. The supercontinuum laser is connected to a SuperK Varia tunable single line filter with centre wavelength from 450 nm up to 790 nm and a variable bandwidth up to 100 nm. The variable centre wavelength makes it ideal for the singlet oxygen experiments, as different photosensitizers have different excitation peaks, usually in the region of 500 nm to 700 nm [2]. The supercontinuum laser is fiber coupled to the optical setup, where the delivery fiber is connected to a collimation package that collects the light and sends it through short-pass filtering which is consisted of two short-pass filters, the first (FESH0950- Thorlabs) with wavelength transmission allowance from 500 nm up to 950 nm and a heat absorbing glass (KG-1 – Edmund Optics) transmitting photons from 400 nm up to 1 μm. The visible light is then reflected by a dichroic mirror (DMLP950- Thorlabs) with 950 nm cut-off wavelength, directing it via an off-axis parabolic mirror (50 mm focal length, MPD129-P01- Thorlabs) to the photosensitizer cuvette with 13.63 μm spot size diameter and 0.146 W/ mm^2 power density at 520 nm wavelength, 0.204 W/ mm^2 at 540 nm, and 0.248 W/ mm^2 at 660 nm, while the total power reaching the cuvette is 1.2 mW at 520 nm wavelength, 1.4 mW at 540 nm and 1.8 mW at 660 nm. The solid angle subtended by the collection optics is approximately 0.022 Sr. Singlet oxygen 1270 nm photons are emitted from the photosensitizer solution in the cuvette, reflected from the same mirror back to the dichroic mirror, which this time allows the infrared photons to pass through. The infrared light is then filtered by both a long-pass filter (FELH1200 – Thorlabs) that transmits photons of 1200 nm wavelength and above, and a custom made optical band-pass filter (90% transmission at 1270 nm, Omega optical) that only allows 1270 nm photons to pass through. A reflective collimation package that is connected to a collection optical fiber routes the photons onto the SNSPD. The parabolic mirrors ensure that the focal length of the collection and illumination is the same, for optimum overlap. It also ensures that as the wavelength is changed (in either illumination or collection beam paths), the optical system does not vary. The overall

optical head size is 20 cm × 15 cm × 5 cm, however, it is not yet optimized for size and could be made much smaller, down to the size of a pen, without sacrificing collection efficiency.

The detector used is a SNSPD consisting of a 7.5 nm thick niobium titanium nitride (NbTiN) film patterned into a 100 nm wide meandering nanowire with 200 nm repeat period covering a 15 μm × 15 μm square area, coupled to a 9 μm diameter core optical fiber. The nanowire was patterned on top of Si substrate and a 240 nm thick SiO_2 layer, while the nanowire was covered by an optical cavity consisting of a layer of 250 nm thick SiO and a 100 nm thick Ag mirror. This simple cavity design gives broadband absorption enhancement in the superconducting nanowire layer in the 1250–2000 nm wavelength range [22]. The SNSPD was characterized using a gain-switched diode laser operating at 1310 nm wavelength (close to 1270 nm singlet oxygen photons), showing a system detection efficiency of ∼25% at 1000 dark counts per second. For both increased signal-to-noise ratio and to keep the overall count rate of the detector below 10% of the laser repetition rate, the detector was operated at reduced bias current, showing sub-Hz dark count rate, while the efficiency remained high enough (∼10–15%) for detection of the singlet oxygen single photon signal. For the cooling of the superconducting detector a Sumitomo RDK-101D Gifford McMahon cold head was used along with a Sumitomo CNA-11C indoor air-cooled compressor [23]. The operation temperature of the SNSPD was stabilized at 3.0 K.

Time correlated single photon counting (TCSPC) is achieved by employing a PicoQuant HydraHarp 400 counter with minimum time bin width of 1 ps. The start signal is given by the supercontinuum laser through an electrical synchronization pulse, while the amplified output from the detector acts as a stop signal. Since the supercontinuum laser runs at a constant repetition rate, the laser pulses are related to the detection events and histograms are generated.

III. Singlet Oxygen Detection

A. Chemicals

For the SOLD measurements we used three different model photosensitizers in solution: Rose Bengal (RB), an organic dye molecule in the xanthene class, used for efficient excitation of oxygen, with strong absorbance at ∼540 nm, high triplet energy and quantum yield in the order of 75% [2], [24], Methylene Blue (MB), a phenothiazinium dye with strong absorbance at 550–700 nm (the selected excitation wavelength for the measurements using MB was 660 nm) and a quantum yield of 52% [2], [24], and Eosin Y (EY), also a xanthene dye with a high excitation peak at 520 nm and a quantum yield of up to 57% [2], [25]. All three photosensitizers were purchased from Sigma-Aldrich. Their molecular weight was 1017.64 for Rose Bengal, 319.85 (anhydrous basis) for Methylene Blue and 647.89 for the Eosin Y, while their molecular structure is shown in Fig. 3. The solutions were prepared by dissolving the photosensitizer powder in distilled water, ethanol and methanol with mass concentrations of 1 mg/ml, with only one exception: The Rose Bengal in distilled water where the selected mass concentration was 500 μg/ml.

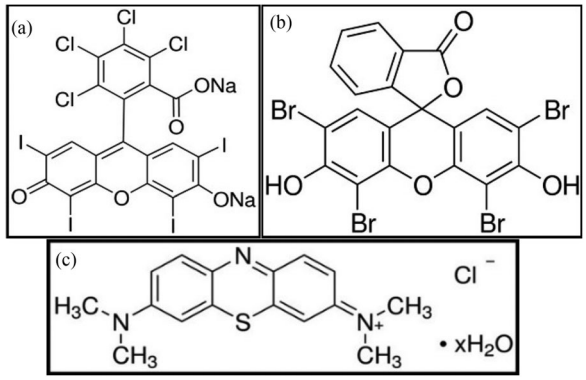

Fig. 3. Molecular structure of (a) rose Bengal, (b) eosin Y, and (c) methylene blue.

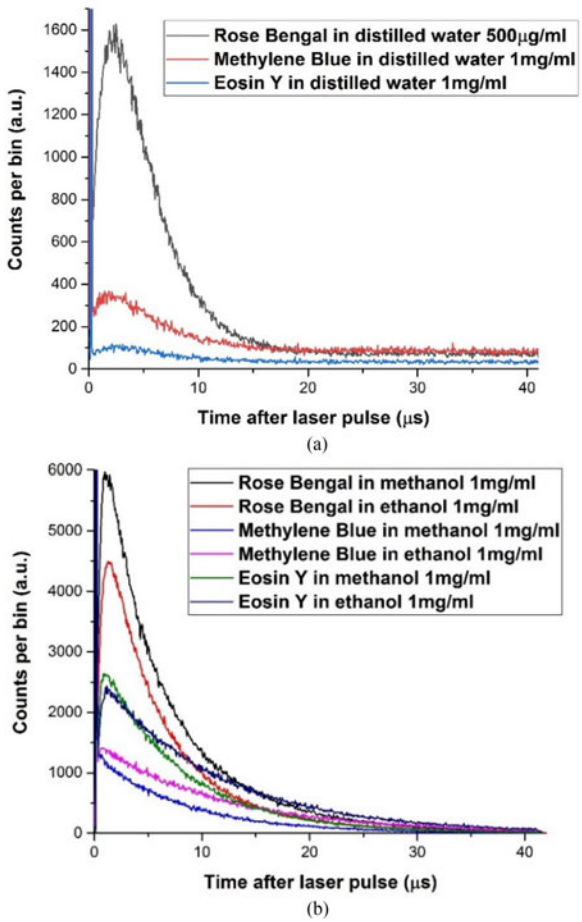

Fig. 4. 1270 nm $^1O_2$ luminescence signal example histograms from RB, MB and EY dissolved in (a) distilled water, and (b) methanol and ethanol. Both histograms were acquired over 10 min and have the same bin width (65536 ps).

B. Singlet Oxygen Luminescence Signal and Lifetimes of Different Photosensitizers

Fig. 4 shows histograms comparing the 1270 nm singlet oxygen signal acquired from Rose Bengal, Methylene Blue and Eosin Y solutions using distilled water as the solvent or other organic solvents such as ethanol and methanol. Acquisition times for all histograms were 10 minutes (600 seconds) and the bin width was 65536 ps.

TABLE I
COMPARISON OF MEASURED LIFETIMES FOR ROSE BENGAL, METHYLENE BLUE, AND EOSIN Y IN DISTILLED WATER

	Rose Bengal in water	Methylene Blue in water	Eosin Y in water
Singlet oxygen lifetime (μs), τ_D	3.12 ± 0.02	4.08 ± 0.04	3.61 ± 0.11
PS triplet state lifetime (μs), τ_T	1.77 ± 0.02	1.70 ± 0.08	1.99 ± 0.20

TABLE II
COMPARISON OF MEASURED LIFETIMES FOR ROSE BENGAL, METHYLENE BLUE, AND EOSIN Y IN ETHANOL

	Rose Bengal in ethanol	Methylene Blue in ethanol	Eosin Y in ethanol
Singlet oxygen lifetime (μs), τ_D	4.215 ± 0.005	11.712 ± 0.007	**10.885 ± 0.005**
PS triplet state lifetime (μs), τ_T	0.42 ± 0.05	0.13 ± 0.10	**0.298 ± 0.003**

Photosensitizer solutions with Rose Bengal dissolved in either distilled water, ethanol or methanol produce higher $^1O_2$ luminescence signals as expected, due to higher $^1O_2$ quantum yield. For the other two photosensitizers, Methylene Blue shows a stronger signal peak when dissolved in distilled water than Eosin Y, with the latter being much more efficient when dissolved in organic solvents. The equation relating the lifetime of singlet oxygen and photosensitizer's triplet state with the generation of the $^1O_2$ in the presence of the illumination, the photosensitizer and the molecular oxygen is shown in (1) [3], [19]:

$$\left[{}^1O_2\right]\ (t) = N\sigma\left[S_0\right]\Phi_D \frac{\tau_D}{\tau_T - \tau_D}\left(\exp\left(\frac{-t}{\tau_T}\right) - \exp\left(\frac{-t}{\tau_D}\right)\right) \quad (1)$$

Where $[^1O_2]$ (t) is the singlet oxygen concentration a time t after the illumination pulse, N is the illumination photons per pulse, σ is the photosensitizer absorption cross-section, S_0 the concentration of the photosensitizer, Φ_D the singlet oxygen quantum yield, τ_D is the singlet oxygen lifetime and τ_T the lifetime of the photosensitizer triplet-state. Both lifetimes are related to the illumination source and the concentrations of oxygen and photosensitizer, making them strongly dependent on their local microenvironment [3], [19].

Both lifetimes, τ_D and τ_T were extracted by fitting these histograms acquired at 1270 nm wavelength, as in our other papers [18], [19]. $^1O_2$ lifetimes τ_D, for Methylene Blue and Eosin Y are longer than those of Rose Bengal regardless of the fact that they have a weaker $^1O_2$ luminescence signal, as shown in Table I, Table II and Table III. For the photosensitizers dissolved in distilled water the longer $^1O_2$ lifetime is observed in Methylene Blue, followed by Eosin Y and then the Rose Bengal. A similar trend is observed for the solutions with the organic solvents, with Methylene Blue and Eosin Y having much longer $^1O_2$ lifetimes than Rose Bengal. Regarding the triplet state lifetimes

TABLE III
COMPARISON OF MEASURED LIFETIMES FOR ROSE BENGAL, METHYLENE BLUE, AND EOSIN Y IN METHANOL

	Rose Bengal in methanol	Methylene Blue in methanol	Eosin Y in methanol
Singlet oxygen lifetime (μs), τ_D	2.70 ± 0.01	7.92 ± 0.01	**7.401 ± 0.003**
PS triplet state lifetime (μs), τ_T	0.29 ± 0.05	0.1 ± 0.2	**0.25 ± 0.02**

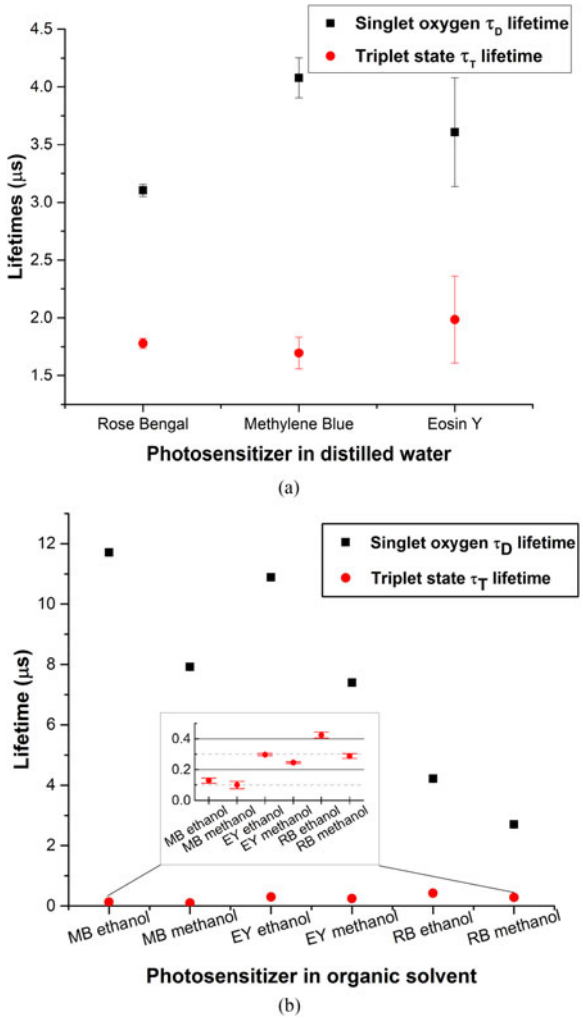

Fig. 5. Comparison of $^1O_2$ lifetime (τ_D) and PS triplet state lifetime (τ_T) for each one of the photosensitizers in (a) distilled water and, (b) ethanol and methanol. Inset plot shows the triplet state lifetimes on a separate Y-axis.

τ_T, all three photosensitizers have similar triplet state lifetimes, taking into consideration the error for each one of these lifetime measurements. While the $^1O_2$ lifetime increases dramatically when the PS is dissolved in an organic solvent, the triplet state lifetime, on the other hand, is decreased to sub-microsecond, showing how the two lifetimes are affected by the environment the photosensitizer and the singlet oxygen are in. Fig. 5 shows a comparison between $^1O_2$ lifetimes τ_D and photosensitizer triplet state lifetimes τ_T for Rose Bengal, Methylene Blue and Eosin Y in distilled water, ethanol and methanol.

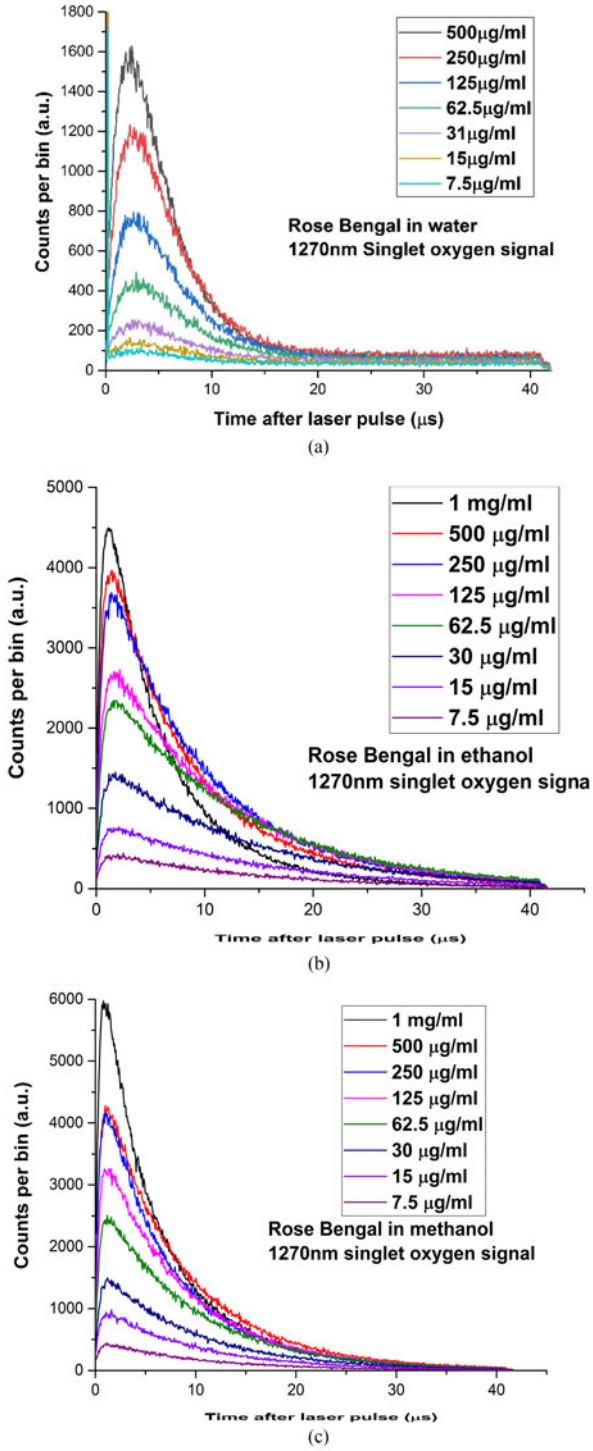

Fig. 6. Comparison histograms of 1270 nm $^1O_2$ luminescence signal by rose Bengal in (a) distilled water, (b) ethanol, and (c) methanol at various mass concentrations. Luminescence signal appears to drop with smaller mass concentrations, while the $^1O_2$ lifetime becomes longer.

C. Singlet Oxygen Luminescence Detection in Different Concentrations

Further experiments were conducted over different concentrations of Rose Bengal solutions with distilled water, ethanol and methanol serving as the solvent. Rose Bengal was preferred from the other two photosensitizers as the one with the highest quantum yield and therefore the strongest $^1O_2$ luminescence signal. For the Rose Bengal solutions dissolved in distilled water, 7 different mass concentrations were tested starting from 500 μg/ml and diluting by half each time ending at 7.5 μg/ml, while for solutions dissolved in the organic solvents the initial mass concentration was 1 mg/ml and the last one at 7.5 μg/ml, resulting in 8 different mass concentration points. Fig. 6 shows comparison histograms of 1270 nm $^1O_2$ luminescence signal produced by Rose Bengal in distilled water, ethanol and methanol at different mass concentrations. Histograms were acquired over 10 minutes with the same bin width and solution volume in the cuvette was 3.5 ml for all the measurements.

TABLE IV
SIGNAL AMPLITUDE (TOTAL COUNTS PER HISTOGRAM) OVER CONCENTRATION FOR ROSE BENGAL IN DISTILLED WATER, METHANOL AND ETHANOL

	Rose Bengal in water	Rose Bengal in methanol	Rose Bengal in ethanol
7.5 µg/ml	29085	70583	**92535**
15 µg/ml	37135	149447	**170220**
30 µg/ml	53414	233106	**308709**
62.5 µg/ml	83845	383140	**484161**
125 µg/ml	120585	472741	**511763**
250 µg/ml	172868	520779	**596601**
500 µg/ml	192041	590416	**567176**
1000 µg/ml	-	636115	**477190**

In these time-resolved experiments, it is clear that as the photosensitizer concentration is reduced the $^1O_2$ phosphorescence signal at 1270 nm weakens to a concentration point where the luminescence signal is almost vanished. In Table IV, a comparison is made between the singlet oxygen signal amplitude for Rose Bengal in distilled water, methanol and ethanol over various mass concentrations. For Rose Bengal in distilled water and methanol the signal amplitude seems to increase with higher photosensitizer concentrations from the lowest mass concentration at 7.5 μg/ml all the way up to the highest concentration for each solution (500 μg.ml for Rose Bengal in water and 1 mg/ml for Rose Bengal in ethanol), with the increase in the signal amplitude between the concentrations not being proportional. For the Rose Bengal in the ethanol solution, the same trend is observed with the difference that its signal amplitude reaches its peak at 250 μg/ml and then is steadily decreased, regardless of the fact that the peak of its singlet oxygen signal in the histogram decay keeps increasing with the higher concentrations. This indicates that apart from the strength of the signal acquired

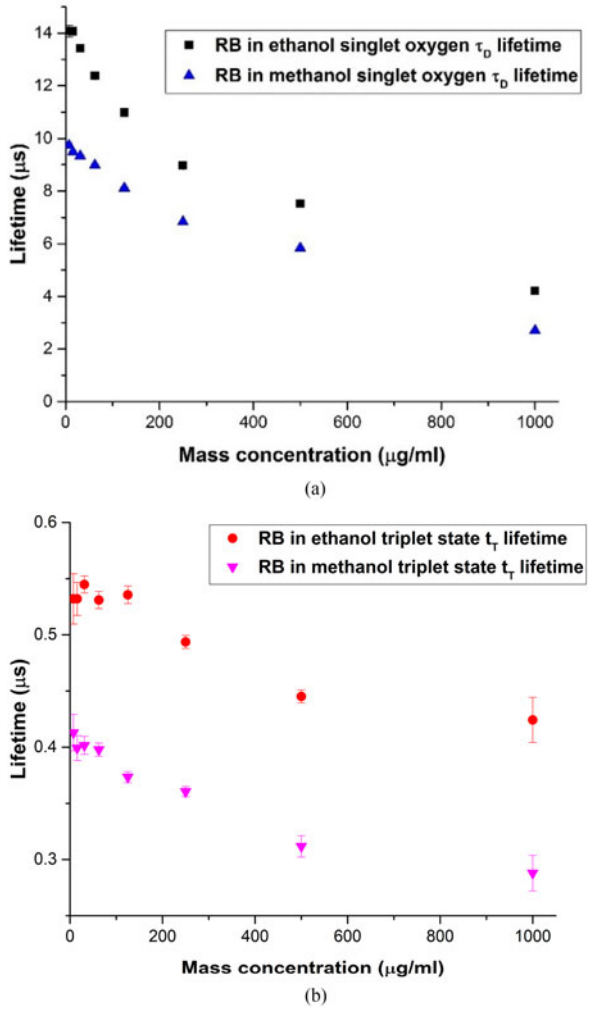

Fig. 7. (a) Comparison of $^1O_2$ lifetime (τ_D) and (b) PS triplet state lifetime (τ_T) for rose Bengal in ethanol and methanol over different mass concentrations. Singlet oxygen lifetime becomes longer as photosensitizer concentration in the solution is smaller, while the photosensitizer triplet state lifetime is barely affected by the reduced concentration of the photosensitizer.

for each photosensitizer concentration, the $^1O_2$ lifetime is also affected by this change. The interaction between the generated singlet oxygen and the photosensitizer molecules is one of the mechanisms that leads to de-excitation of the singlet oxygen. Therefore, the singlet oxygen lifetime appears to be quenched more with higher photosensitizer concentrations, reducing the probability of photon emission. So, as the concentration of the photosensitizer in the solution gets higher, the singlet oxygen lifetime τ_D appears to be significantly shorter, while triplet state lifetime τ_T seems not to be affected much, as shown in Fig. 7. This is easier to observe in the case where Rose Bengal is dissolved in ethanol where the luminescence signal is stronger and the singlet oxygen decay is altered more.

IV. Conclusions

An advanced optical system for SOLD studies is presented exploiting the benefits of a supercontinuum laser, an adjustable illumination source suitable for characterizing the majority of the photosensitizers as well as for further SOLD dosimetry experiments. Also, an advanced fiber-coupled optical system greatly assists in efficient singlet oxygen generation and detection. In the next design iteration, we could either miniaturize the optical setup or explore a miniaturized fiber optic probe (following the example [26]) for use in tissue and clinical studies, easy and precise placement of this fiber-coupled sensor head inside the tissue would be a huge benefit, boosting signal and spatial specificity. The SOLD system is completed by an SNSPD with improved system efficiency and reduced down to sub-Hz dark count rate. Further improvements in miniaturized cryogenics for SNSPDs have recently been reported by our group [27]. This improved SOLD system has been carefully benchmarked, offering an enhanced detection of the singlet oxygen luminescence signal at 1270 nm, using three photosensitizers, with different excitation peaks, in solution dissolved in distilled water and organic solvents. The overall performance is significantly improved, while the new components offer a more practical SOLD system that can be easier utilized in direct PDT dosimetry researches *in vitro* animal models and *in vivo* clinical trials.

Acknowledgment

K. Erotokritou would like to thank NICT Japan for hosting him through an internship.

References

[1] P. R. Ogilby, "Singlet oxygen: There is indeed something new under the sun," *Chem. Soc. Rev.*, vol. 39, no. 8, pp. 3181–3209, Aug. 2010.
[2] M. C. DeRosa and R. J. Crutchley, "Photosensitized singlet oxygen and its applications," *Coordination Chem. Rev.*, vol. 233–234, pp. 351–371, Nov. 2002.
[3] C. Schweitzer and R. Schmidt, "Physical mechanisms of generation and deactivation of singlet oxygen," *Chem. Rev.*, vol. 103, no. 5, pp. 1685–1757, Apr. 2003.
[4] P. Mroz, A. Yaroslavsky, G. B. Kharkwal, and M. R. Hamblin, "Cell death pathways in photodynamic therapy of cancer," *Cancers*, vol. 3, no. 2, pp. 2516–2539, Dec. 2011.
[5] T. J. Dougherty *et al.*, "Photodynamic therapy," *J. Natl. Cancer Inst.*, vol. 90, no. 12, pp. 889–905, Jun. 1998.
[6] G. Yu *et al.*, "Noninvasive monitoring of murine tumor blood flow during and after photodynamic therapy provides early assessment of therapeutic efficacy," *Clin. Cancer Res.*, vol. 11, no. 9, pp. 3543–3552, May 2005.
[7] M. T. Jarvi, M. J. Niedre, M. S. Patterson, and B. C. Wilson, "Singlet oxygen luminescence dosimetry (SOLD) for photodynamic therapy: Current status, challenges and future prospects," *Photochem. Photobiol.*, vol. 82, no. 5, pp. 1198–1210, Oct. 2006.
[8] B. C. Wilson, M. S. Patterson, and L. Lilge, "Implicit and explicit dosimetry in photodynamic therapy: A New paradigm," *Lasers Med. Sci.*, vol. 12, no. 3, pp. 182–199, Oct. 1997.
[9] R. A. Weersink *et al.*, "Techniques for delivery and monitoring of TOOKAD (WST09)-mediated photodynamic therapy of the prostate: Clinical experience and practicalities," *J. Photochem. Photobiol.*, vol. 79, no. 3, pp. 211–222, Jun. 2005.
[10] M. S. Thompson *et al.*, "Clinical system for interstitial photodynamic therapy with combined on-line dosimetry measurements," *Appl. Opt.*, vol. 44, no. 19, pp. 4023–4031, Jul. 2005.
[11] T. C. Zhu, J. C. Finlay, and S. M. Hahn, "Determination of the distribution of light, optical properties, drug concentration, and tissue oxygenation *in-vivo* in human prostate during motexafin lutetium-mediated photodynamic therapy," *J. Photochem. Photobiol.*, vol. 79, no. 3, pp. 231–241, Jun. 2005.
[12] H. Zeng, M. Korbelik, D. I. McLean, C. MacAulay, and H. Lui, "Monitoring photoproduct formation and photobleaching by fluorescence spectroscopy has the potential to improve PDT dosimetry with a verteporfin-like photosensitizer," *Photochem. Photobiol.*, vol. 75, no. 4, pp. 398–405, Apr. 2002.

[13] I. Georgakoudi, M. G. Nichols, and T. H. Foster, "The mechanism of Photofrin photobleaching and its consequences for photodynamic dosimetry," *Photochem. Photobiol.*, vol. 65, no. 1, pp. 135–144, Jan. 1997.
[14] J. S. Dysart and M. S. Patterson, "Photobleaching kinetics, photoproduct formation, and dose estimation during ALA induced PpIX PDT of MLL cells under well oxygenated and hypoxic conditions," *Photochem. Photobiol. Sci.*, vol. 5, no. 1, pp. 73–81, Jan. 2006.
[15] A. Molckovsky and B. C. Wilson, "Monitoring of cell and tissue responses to photodynamic therapy by electrical impedance spectroscopy," *Phys. Med. Biol.*, vol. 46, no. 4, pp. 983–1002, Apr. 2001.
[16] D. Lapointe *et al.*, "High-resolution PET imaging for *in-vivo* monitoring of tumor response after photodynamic therapy in mice," *J. Nucl. Med.*, vol. 40, no. 5, pp. 876–882, May 1999.
[17] M. Niedre, M. S. Patterson, and B. C. Wilson, "Direct near-infrared luminescence detection of singlet oxygen generated by photodynamic therapy in cells in vitro and tissues *in vivo*," *Photochem. Photobiol.*, vol. 75, no. 4, pp. 382–391, Apr. 2002.
[18] N. R. Gemmell *et al.*, "Singlet oxygen luminescence detection with a fiber-coupled superconducting nanowire single-photon detector," *Opt. Express*, vol. 21, no. 4, pp. 5005–5013, Feb. 2013.
[19] N. R. Gemmell *et al.*, "A compact fiber-optic probe-based singlet oxygen luminescence detection system," *J. Biophoton.*, vol. 10, no. 2, pp. 320–326, Feb. 2017.
[20] G. Boso *et al.*, "Time-resolved singlet-oxygen luminescence detection with an efficient and practical semiconductor single-photon detector," *Biomed. Opt. Express*, vol. 7, no. 1, pp. 211–224, Dec. 2016.
[21] Robert H. Hadfield, "Single-photon detectors for optical quantum information applications," *Nature Photon.*, vol. 3, pp. 696–705, Dec. 2013.
[22] S. Miki, T. Yamashita, H. Terai, and Z. Wang, "High performance fiber-coupled NbTiN superconducting nanowire single photon detectors with Gifford-McMahon cryocooler," *Opt. Express*, vol. 21, no. 8, pp. 10208–10214, Apr. 2013.
[23] R. H. Hadfield *et al.*, "Singlet photon source characterization with a superconducting single photon detector," *Opt. Express*, vol. 13, no. 26, pp. 10846–10853, Jul. 2005.
[24] R. W. Redmond and J. N. Gamlin, "A compilation of singlet oxygen yields from biologically relevant molecules," *Photochem. Photobiol.*, vol. 70, no. 4, pp. 391–475, Oct. 1999.
[25] F. Amat-Guerri, M. M. C. Lopez-Gonzalez, R. Martinez-Utrilla, and R. Sastre, "Singlet oxygen photogeneration by ionized and un-ionized derivatives of Rose Bengal and Eosin Y in diluted solutions," *J. Photochem. Photobiol A, Chem.*, vol. 53, no. 2, pp. 199–210, Jul. 1990.
[26] G. Williams, T. Euser, P. Russell, A. MacRobert, and A. Jones, "Highly sensitive luminescence detection of photosensitized singlet oxygen within photonic crystal fibre," *ChemPhotoChem*, 2018, doi; 10.1002/cptc.201800028.
[27] N. R. Gemmell *et al.*, "A miniaturized 4 K platform for superconducting infrared photon counting detectors," *Supercond. Sci. Technol.*, vol. 30, no. 11, Sep. 2017, Art. no. 11LT01.

Konstantinos Tsimvrakidis received the B.Sc. degree in electrical engineering from the Technological Institute of Central Greece, Chalcis, Greece, in 2014, and the M.Sc. degree in nanoscience from the University of Strathclyde, Glasgow, U.K., in 2015. He is currently working toward the Ph.D. degree at the University of Glasgow, Glasgow, U.K. His research interest include singlet oxygen luminescence detection with superconducting nanowire single-photon detectors.

Nathan R. Gemmell received the Ph.D. in infrared single photon sensing from Heriot-Watt University, Edinburgh, U.K., and was a Postdoctoral Researcher supported by the QuantIC quantum technology hub with the University of Glasgow, Glasgow, U.K. He is currently an Instrumentation Scientist with the University of Sussex, Brighton, U.K. He carried out the first singlet oxygen luminescence studies with superconducting nanowire single-photon detectors in collaboration with the Ontario Cancer Institute, Toronto, ON, Canada.

Kleanthis Erotokritou received the Bachelor's degree in engineering from the University of Newcastle, Newcastle upon Tyne, U.K., the Master's degree in nanoscience and nanotechnology from the University of Glasgow, Glasgow, U.K., where he is currently working toward the Ph.D. degree with the School of Engineering, focusing on the fabrication of superconducting nanowire devices integrated in advanced optical architectures. In 2017, he completed a three-month research internship with the National Institute for Information and Communications Technology, Kobe, Japan.

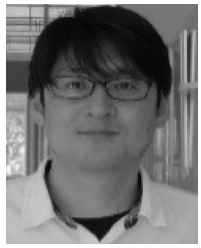

Shigehito Miki received the Ph.D. degree in electrical engineering from Kobe University, Kobe, Japan, in 2002. He is currently a Senior Researcher with the Frontier Research Laboratory, National Institute of Information and Communications Technology, Kobe, Japan. His research interests include superconducting devices and physics and single photon detectors. He is a member of the Japan Society of Applied Physics and the Institute of Electronics, Information and Communication Engineers of Japan.

Masahiro Yabuno received the Ph.D. degree in engineering from Tohoku University, Sendai, Japan, in 2012. In 2012, he joined Research Institute of Electrical Communication, Tohoku University, Japan, where he was engaged in the study of quantum optics. Then, he moved to National Institute of Information and Communications Technology, Japan, in 2016. He is currently engaged in research and development of superconducting single-photon detectors. He is a member of the Japan Society of Applied Physics.

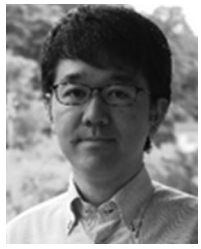

Taro Yamashita received the Ph.D. degree in physics from Tohoku University, Sendai, Japan, in 2005. From 2009 to 2018, he was a Researcher with the National Institute of Information and Communications Technology, Tokyo, Japan. He is currently an Associate Professor with Nagoya University Nagoya, Japan. He is also a PRESTO Researcher with the Japan Science and Technology Agency, Japan. His research interests include superconducting electronics and spintronics. He is a member of the Japan Society of Applied Physics, the Physical Society of Japan, and the Institute of Electronics, Information, and Communication Engineers of Japan.

Hirotaka Terai received the Ph.D. degree in electronics engineering from Nagoya University, Nagoya, Japan, in 1996. From 1996 to 1997, he was a Researcher with the Fundamental Research Laboratories of NEC Co. Ltd. In 1997, he joined the Communications Research Laboratories in Ministry of Posts and Telecommunication. He is currently an Executive Researcher with the National Institute of Information and Communications Technology, Kobe, Japan. His research interests include superconducting detectors and digital circuits. He is a member of the Japan Society of Applied Physics and the Institute of Electronics, Information, and Communication Engineers of Japan.

Robert H. Hadfield (SM'13) is a Professor of photonics and Head of the Division of Electronics and Nanoscale Engineering with the School of Engineering, the University of Glasgow, Glasgow, U.K. He has authored or co-authored more than 80 papers on superconducting devices and advanced photon counting techniques. He holds a European Research Council Consolidator Grant. He is a Fellow of the Optical Society of America.